

Interactions among HCLS1, HAX1 and LEF-1 proteins are essential for G-CSF-triggered granulopoiesis

Julia Skokowa¹, Maxim Klimiankou^{1,8}, Olga Klimenkova^{1,8}, Dan Lan^{1,2}, Kshama Gupta¹, Kais Hussein³, Esteban Carrizosa⁴, Inna Kusnetsova¹, Zhixiong Li⁵, Claudio Sustmann⁷, Arnold Ganser⁶, Cornelia Zeidler¹, Hans-Heinrich Kreipe³, Janis Burkhardt⁴, Rudolf Grosschedl⁷ & Karl Welte¹

We found that hematopoietic cell-specific Lyn substrate 1 (HCLS1 or HS1) is highly expressed in human myeloid cells and that stimulation with granulocyte colony-stimulating factor (G-CSF) leads to HCLS1 phosphorylation. HCLS1 binds the transcription factor lymphoid-enhancer binding factor 1 (LEF-1), transporting LEF-1 into the nucleus upon G-CSF stimulation and inducing LEF-1 autoregulation. In patients with severe congenital neutropenia, inherited mutations in the gene encoding HCLS1-associated protein X-1 (HAX1) lead to profound defects in G-CSF-triggered phosphorylation of HCLS1 and subsequently to reduced autoregulation and expression of LEF-1. Consistent with these results, HCLS1-deficient mice are neutropenic. In bone marrow biopsies of the majority of tested patients with acute myeloid leukemia, HCLS1 protein expression is substantially elevated, associated with high levels of G-CSF synthesis and, in some individuals, a four-residue insertion in a proline-rich region of HCLS1 protein known to accelerate intracellular signaling. These data demonstrate the importance of HCLS1 in myelopoiesis *in vitro* and *in vivo*.

HCLS1 contains a Src homology 3 (SH3) adapter domain and can initiate activation of receptor-coupled tyrosine kinases^{1–3}. Phosphorylation of HCLS1, mediated by tyrosine kinases such as Syk, Lyn and Lck and adapter proteins such as Grb2 (refs. 2–9), leads to its activation. In particular, phosphorylation of HCLS1 on Tyr397 by Syk and Lyn leads to HCLS1 translocation into the nucleus^{10,11}. The helix-turn-helix repeat and coiled-coil domains of HCLS1 are required for its binding to F-actin and activation of the Arp2-Arp3 complex^{1–3,11}. High HCLS1 levels are associated with chronic lymphoblastic leukemia^{12,13}, whereas a lack of HCLS1 in lymphocyte precursors leads to defective proliferation and differentiation of B lymphocytes after B cell receptor activation¹⁴. The *HCLS1* gene promoter has binding sites for the granulocyte-specific transcription factors C/EBP α and C/EBP β (ref. 2). However, the role of HCLS1 in G-CSF-triggered myelopoiesis has not been investigated.

G-CSF receptor (G-CSFR) activation upon ligand binding induces myeloid cell proliferation, survival and differentiation^{15–17}. Defects in G-CSFR downstream effectors abrogate myeloid differentiation and might lead to either leukemic transformation or neutropenia. Several different intracellular signaling systems are activated by G-CSFR, such as Jak-STAT¹⁸, PI3K-Akt^{19,20}, MAPK-ERK²¹ and Nampt-NAD⁺-SIRT1 (ref. 22). G-CSFR does not have intrinsic tyrosine kinase activity; it interacts with and activates cytosolic protein-tyrosine kinases such as Lyn and Syk^{19,20,23–26}, leading to tyrosine phosphorylation of

a set of positive and negative adapters and effectors. Under defined conditions, phosphorylated HCLS1 is also associated with Lyn and Syk^{4,6,8,10}; hence we hypothesized that HCLS1 might be involved in G-CSFR signaling.

Severe congenital neutropenia is a hematopoietic syndrome associated with defective G-CSFR signaling and characterized by a ‘maturation arrest’ of granulopoiesis at the promyelocyte stage^{27,28}. Recently, we described mutations in *HAX1*, encoding HCLS1-associated protein X-1 (HAX1), for a subgroup of patients with congenital neutropenia²⁹. HAX1 is a ubiquitously expressed protein^{29–33}, but the definitive effects of *HAX1* mutations that lead to ineffective granulopoiesis but no other abnormalities in congenital neutropenia are still unclear. We previously identified LEF-1 as an essential trigger of granulocytic differentiation³⁴. LEF-1 controls the proliferation, lineage commitment and granulocytic differentiation of hematopoietic stem cells via activation of C/EBP α (ref. 34). In patients with congenital neutropenia who have *HAX1* mutations, LEF-1 expression is reduced and its function is impaired³⁴, indicating that HAX1-associated signaling is involved in the regulation of LEF-1 in myeloid cells. LEF-1 belongs to the LEF-1 T-cell factor (TCF) family of high mobility group domain-containing transcription factors^{35,36}. LEF-1 can activate target genes only in association with other binding partners, such as β -catenin^{35–40}. Fine-tuning of LEF-1 expression is indispensable for proper regulation of the proliferation and differentiation of

¹Department of Molecular Hematopoiesis, Hannover Medical School, Hannover, Germany. ²Department of Pediatrics, The First Affiliated Hospital of GuangXi Medical University, NanNing, China. ³Department of Pathology, Hannover Medical School, Hannover, Germany. ⁴Department of Pathology and Laboratory Medicine, Children's Hospital of Philadelphia and University of Pennsylvania School of Medicine, Philadelphia, Pennsylvania, USA. ⁵Institute of Experimental Hematology, Hannover Medical School, Hannover, Germany. ⁶Department of Hematology, Hemostasis, Oncology and Stem Cell Transplantation, Hannover Medical School, Hannover, Germany. ⁷Max Planck Institute of Immunobiology, Department of Cellular and Molecular Immunology, Freiburg, Germany. ⁸These authors contributed equally to this work. Correspondence should be addressed to J.S. (skokowa.julia@mh-hannover.de) or K.W. (Welte.Karl.H@mh-hannover.de).

Received 6 March; accepted 27 August; published online 23 September 2012; doi:10.1038/nm.2958

myeloid cells. Thus, lack of LEF-1 expression causes defective granulopoiesis in congenital neutropenia³⁴, and elevated levels of constitutively active LEF-1 lead to hyperproliferation of myeloid progenitors and development of acute myeloid leukemia (AML)^{34,41}. LEF-1 activates granulopoiesis independently of β -catenin³⁴. Myeloid-specific interaction partners of LEF-1 and the mechanisms by which LEF-1 expression is deregulated in patients with congenital neutropenia are unknown. Analysis of the pathological events downstream of HAX1 mutations may help to answer these questions.

RESULTS

HCLS1 protein interacts with LEF-1 protein

To identify hematopoietic-specific interaction partners of LEF-1, we carried out *in silico* analysis of LEF-1 protein using ScanSite software^{42,43} to identify motifs within the protein that are likely to bind other proteins. LEF-1 protein has a highly conserved HCLS1-binding site in the context-dependent domain at Pro191 (Fig. 1a). HCLS1 was most highly expressed in myeloid cells compared with other lineages, as shown in a micrograph of a bone marrow section where myeloid cells and segmented granulocytes showed abundant HCLS1 staining (Fig. 1b).

To confirm the binding of HCLS1 to LEF-1, we carried out immunoprecipitation experiments in HEK293T cells transfected with HCLS1 cDNA together with LEF-1 cDNA or mutant LEF-1 protein (LEF-1 Ala16), in which residues 186–192 were replaced by an alanine-glycine sequence to eliminate the putative HCLS1-binding site. HCLS1 co-precipitated with wild-type (WT) LEF-1, but not with the LEF-1

Ala16 mutant (Fig. 1c). We also detected an interaction between endogenous LEF-1 and HCLS1 proteins in lysates from the Jurkat cell line, which highly expresses HCLS1 and LEF-1 (Fig. 1d).

We confirmed the interaction between native LEF-1 and HCLS1 proteins by blue native gel electrophoresis (BN-PAGE; first dimension) followed by identification of the proteins within the single protein complexes using SDS-PAGE (second dimension) and western blotting. We detected HCLS1, LEF-1, dominant-negative LEF-1 (dnLEF-1, which lacks the β -catenin-binding domain) and HAX1 in a single complex (Fig. 1e). HAX1 was also found in a complex with LEF-1 in LEF-1-transfected HEK293T cells (Supplementary Fig. 1a). In a pull-down assay using lysates from Jurkat cells, LEF-1 protein was pulled down by GST-HCLS1 protein but not by GST (Fig. 1f). These data strongly support the existence of a direct interaction between HCLS1 and LEF-1.

HCLS1 is associated with Syk, Lyn and LEF-1 in CD34⁺ cells

HCLS1 is known to be activated by phosphorylation upon treatment with hematopoietic cytokines such as erythropoietin⁶. Therefore, we analyzed whether stimulation of hematopoietic cells with G-CSF leads to HCLS1 phosphorylation. Indeed, *in vitro* G-CSF stimulation of human CD34⁺ cells showed time-dependent phosphorylation of HCLS1 protein on Tyr397 (Supplementary Fig. 2a and Fig. 1g), leading to enhanced interaction with LEF-1 (Fig. 1h and data not shown). Mutation of the Tyr397 residue in the HCLS1 protein led to reduced binding of HCLS1 to LEF-1 (data not shown).

Although the association between HCLS1 with Lyn in nonstimulated CD34⁺ cells was weak, it was apparent after 30 min of G-CSF

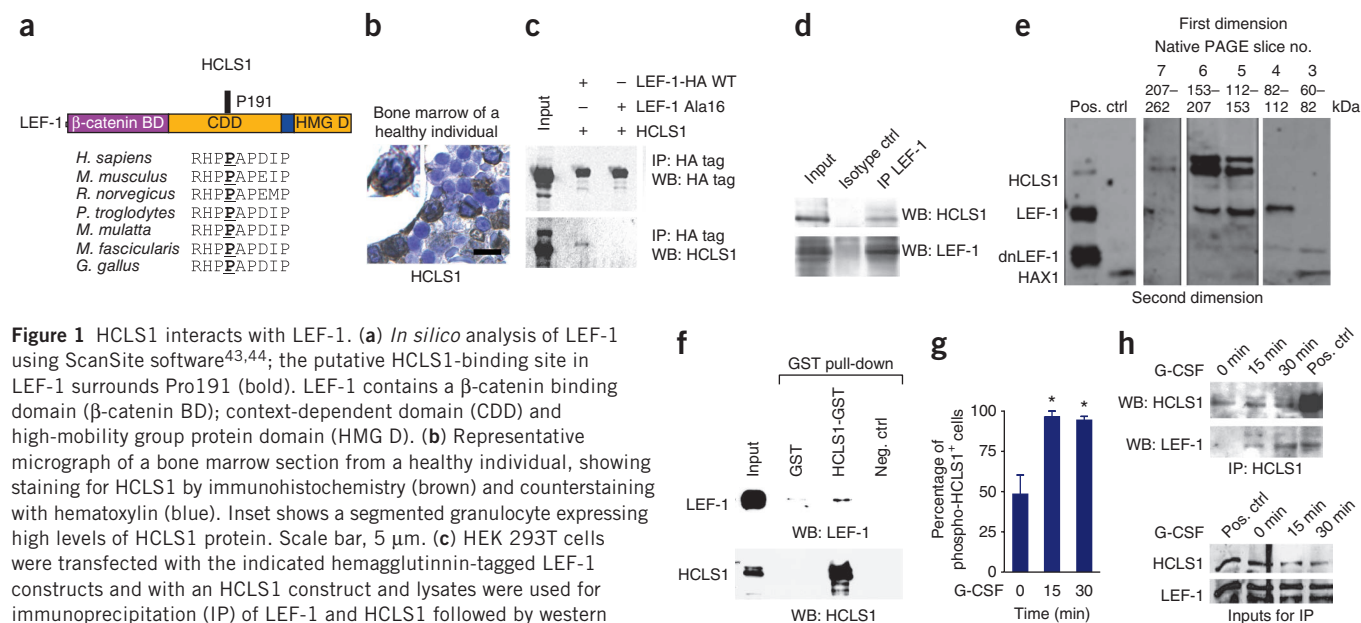


Figure 1 HCLS1 interacts with LEF-1. (a) *In silico* analysis of LEF-1 using ScanSite software^{43,44}; the putative HCLS1-binding site in LEF-1 surrounds Pro191 (bold). LEF-1 contains a β -catenin binding domain (β -catenin BD); context-dependent domain (CDD) and high-mobility group protein domain (HMG D). (b) Representative micrograph of a bone marrow section from a healthy individual, showing staining for HCLS1 by immunohistochemistry (brown) and counterstaining with hematoxylin (blue). Inset shows a segmented granulocyte expressing high levels of HCLS1 protein. Scale bar, 5 μ m. (c) HEK 293T cells were transfected with the indicated hemagglutinin-tagged LEF-1 constructs and with an HCLS1 construct and lysates were used for immunoprecipitation (IP) of LEF-1 and HCLS1 followed by western blotting of the immunoprecipitates using the indicated antibodies. The isotype control used for IP was negative (not shown). HA, hemagglutinin. (d) Representative western blot of LEF-1 immunoprecipitates from Jurkat cells using the indicated antibodies. (e) The interaction between native LEF-1 and HCLS1 was analyzed by isolating complexes on BN-PAGE (first dimension) followed by identification of proteins within the complexes by SDS-PAGE (second dimension) and western blotting for HCLS1, LEF-1, dnLEF-1 and HAX1. Shown are representative images of BN-PAGE with marker and Jurkat cell lysates as a positive control (left) and of western blot of complexes isolated from slices 3–7 of BN-PAGE (right). (f) Following pull-down assays of Jurkat cell lysates using human recombinant HCLS1-GST-tagged protein or GST protein, representative western blots are shown using antibodies to LEF-1 and HCLS1. (g) CD34⁺ bone marrow cells from two healthy individuals were treated with 10 ng ml⁻¹ G-CSF. At the indicated time points, total and phospho-HCLS1 proteins were quantified using FACS analysis. Shown is the percentage of phospho-HCLS1⁺ cells in the HCLS1⁺ cell population. Data are mean \pm s.d. and are derived from three independent experiments, each in duplicate, **P* < 0.05. (h) Endogenous HCLS1 from primary bone marrow CD34⁺ cells treated or untreated with 10 ng ml⁻¹ G-CSF for the indicated lengths of time was immunoprecipitated with antibody to HCLS1. Coimmunoprecipitates of LEF-1 and HCLS1 were detected by western blotting. Shown are representative western blot images of immunoprecipitates (top) and of the inputs used for immunoprecipitation (bottom); the isotype control for IP was negative (not shown). Lysate of untreated CD34⁺ cells was used as a positive control.

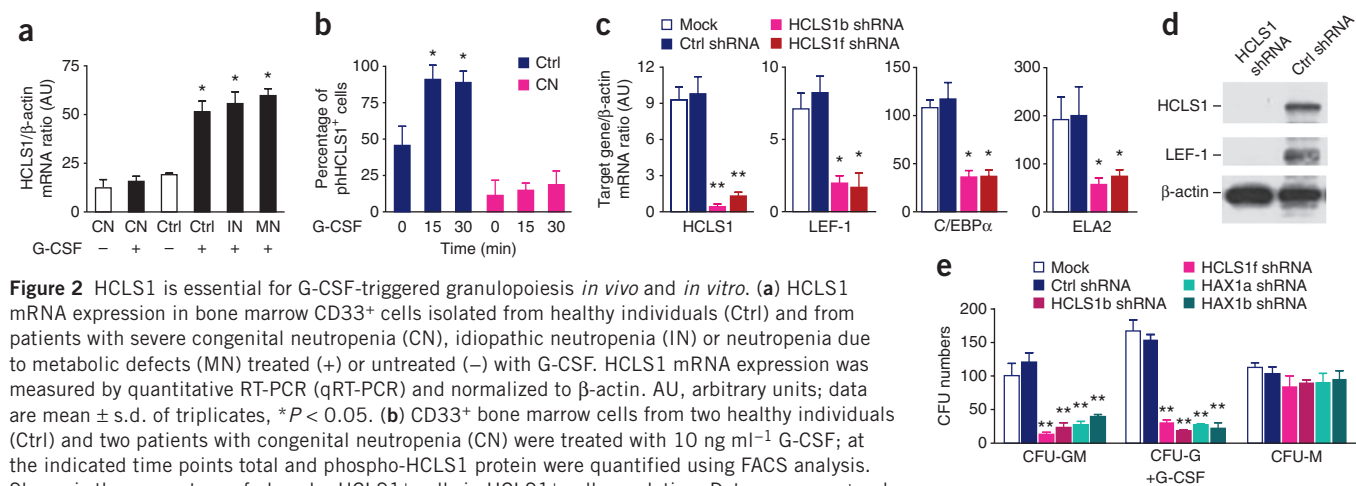


Figure 2 HCLS1 is essential for G-CSF-triggered granulopoiesis *in vivo* and *in vitro*. (a) HCLS1 mRNA expression in bone marrow CD33⁺ cells isolated from healthy individuals (Ctrl) and from patients with severe congenital neutropenia (CN), idiopathic neutropenia (IN) or neutropenia due to metabolic defects (MN) treated (+) or untreated (-) with G-CSF. HCLS1 mRNA expression was measured by quantitative RT-PCR (qRT-PCR) and normalized to β -actin. AU, arbitrary units; data are mean \pm s.d. of triplicates, * $P < 0.05$. (b) CD33⁺ bone marrow cells from two healthy individuals (Ctrl) and two patients with congenital neutropenia (CN) were treated with 10 ng ml⁻¹ G-CSF; at the indicated time points total and phospho-HCLS1 protein were quantified using FACS analysis. Shown is the percentage of phospho-HCLS1⁺ cells in HCLS1⁺ cell population. Data are mean \pm s.d. and are derived from three independent experiments, each in duplicate, * $P < 0.05$. (c–e) CD34⁺ cells from healthy individuals ($n = 3$) were transduced with the indicated constructs and RFP⁺ cells were sorted on day 4 of culture. Two different shRNA constructs, HCLS1b and HCLS1f, targeting two different regions of HCLS1 mRNA, were used. Mock indicates untransduced cells cultured in the same conditions as transduced cells. (c) Expression of the indicated mRNAs was assessed using qRT-PCR. Data are mean \pm s.d. and are derived from three independent experiments, each in triplicate, * $P < 0.05$, ** $P < 0.01$. (d) Western blot analysis of HCLS1 and LEF-1. β -actin was used as a loading control. (e) The indicated CFU assays were performed. Data are mean \pm s.d. and are derived from three independent experiments, each in duplicate, ** $P < 0.01$.

stimulation (**Supplementary Fig. 2b**). Moreover, although Syk constitutively interacted with HCLS1, the amount of HCLS1 bound to Syk was higher at 30 min of G-CSF stimulation as compared to control cells (**Supplementary Fig. 2b**).

We recently reported that G-CSF induces granulopoiesis via upregulation of the Nampt-NAD⁺-SIRT1 pathway²². Consistent with the results of that report, treatment of healthy individuals with the Nampt substrate nicotinamide led to a substantial upregulation of HCLS1 mRNA expression in bone marrow CD34⁺ and CD33⁺ cells, and treatment of CD34⁺ cells from healthy individuals with Nampt or G-CSF also led to a substantial upregulation of HCLS1 mRNA expression (**Supplementary Fig. 3a,b**).

HCLS1 is essential for G-CSF-triggered myelopoiesis

We previously identified *HAX1* mutations in a group of patients with congenital neutropenia leading to an absence of HAX1 protein²⁹. Notably, in CD33⁺ granulocytic progenitors from patients with congenital neutropenia harboring *HAX1* mutations, G-CSF treatment did not upregulate HCLS1 mRNA expression, as compared to cells from healthy volunteers and patients with idiopathic or metabolic neutropenia (**Fig. 2a** and **Supplementary Fig. 4b**). In contrast, HAX1 mRNA levels were similar between the studied groups (**Supplementary Fig. 4a,b**). Similar to our previous observations³⁴, and in line with lower expression of HCLS1 mRNA in congenital neutropenia, LEF-1 mRNA and protein expression were much lower in CD33⁺ cells from such patients as compared with the other groups (**Supplementary Fig. 4c**). Amounts of total and phospho-HCLS1 proteins were also lower in G-CSF-treated CD33⁺ myeloid progenitors from patients with congenital neutropenia (**Fig. 2b** and **Supplementary Fig. 5a**). In CD34⁺ cells from healthy individuals, HAX1 knockdown blocked HCLS1 phosphorylation following G-CSF treatment (**Supplementary Fig. 5b–d**).

CD34⁺ cells transduced with HCLS1- or HAX1-specific shRNA and treated with G-CSF showed lower mRNA levels of LEF-1 target genes (encoding *C/EBP α* and *ELA2*, which are myeloid specific, as well as encoding cyclin D1 and survivin) but unchanged mRNA levels of other TCF family proteins and other proteins in the Nampt-SIRT

pathway (*TCF-3* and *TCF-4*, *Nampt*, *SIRT1* and *C/EBP β*), as compared with mock or control shRNA-transduced cells (**Fig. 2c,d**, **Supplementary Figs. 6a,b** and **7a** and data not shown). Microarray analysis showed downregulation of members of the Wnt signaling cascade in HCLS1-deficient CD34⁺ cells, as compared with control shRNA-transduced cells (**Supplementary Table 1**).

We further analyzed the involvement of HCLS1 and HAX1 in G-CSF-induced granulocytic differentiation of CD34⁺ bone marrow cells of healthy individuals by a colony-forming unit (CFU) assay. After knockdown of HCLS1 or HAX1, *in vitro* granulocytic differentiation of CD34⁺ cells was significantly reduced (**Fig. 2e** and **Supplementary Fig. 8a,b**), but the number of erythroid colonies (BFU-E) was only slightly reduced (**Supplementary Fig. 8c**). Knockdown of HCLS1 or HAX1 also inhibited ATRA-triggered differentiation of the NB4 promyelocytic cell line (**Supplementary Fig. 9a–c**). These results indicate that HCLS1 and HAX1 are essential for granulocytic differentiation *in vitro*.

HCLS1 affects LEF-1 nuclear translocation and activation

To evaluate the mechanisms of LEF-1 activation by HCLS1 in primary CD34⁺ cells, we first analyzed whether HCLS1 is involved in intracellular transport of the LEF-1 protein. We transduced CD34⁺ cells with a lentiviral construct expressing WT LEF-1 cDNA or LEF-1 cDNA with a mutated HCLS1-binding site (LEF-1 Ala16). After treatment of the cells with G-CSF for 15 min, WT LEF-1 but not LEF-1 Ala16 was predominantly localized in the nucleus (**Fig. 3a**), suggesting a key role of HCLS1 in the nuclear transport of LEF-1.

In the next set of experiments, we knocked down endogenous HCLS1 in CD34⁺ cells; transduced the cells with cDNA encoding WT HCLS1, HCLS1 with a mutated nuclear localization signal (HCLS1 NLS) or HCLS1 with mutated Tyr397 (HCLS1 Y397F); treated the cells with G-CSF for 15 min; and evaluated the intracellular localization of LEF-1 and of LEF-1–HCLS1 and LEF-1–phospho-HCLS1 complexes using the Duolink *in situ* proximity ligation assay (PLA)^{44–46}. In cells expressing WT HCLS1, G-CSF induced nuclear translocation of LEF-1. However, in the presence of HCLS1 Y397F or HCLS1 NLS, LEF-1 did not translocate to the nucleus (**Fig. 3b**). Moreover, we

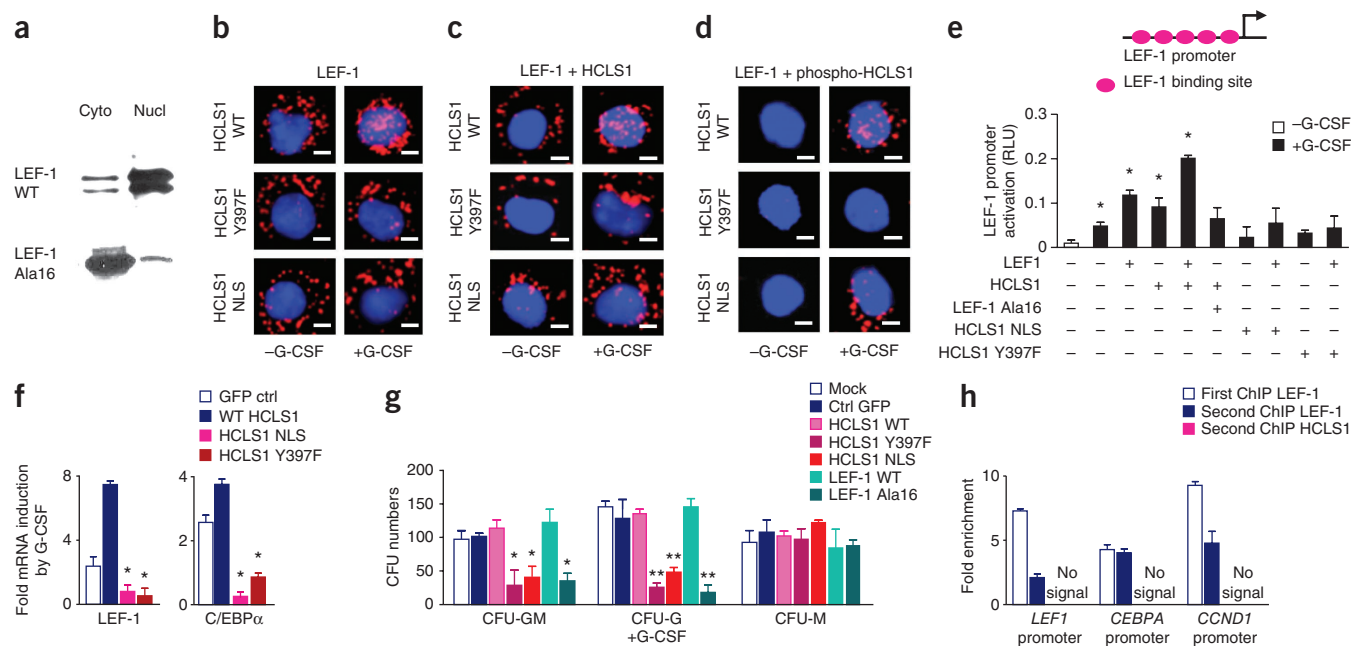


Figure 3 HCLS1 and HAX1 are involved in nuclear transport, activation and autoregulation of LEF-1. **(a)** Western blot analysis of cytoplasmic (cyto) and nuclear (nucl) lysates of CD34⁺ cells transduced with lentiviral constructs expressing WT LEF-1 cDNA or LEF-1 Ala16 cDNA and treated with G-CSF for 15 min after starvation for 12–14 h. **(b–d)** Intracellular localization of LEF-1 **(b)**, LEF-1–HCLS1 complexes **(c)** and LEF-1–phospho-HCLS1 complexes **(d)** in CD34⁺ cells using the Duolink *in situ* PLA assay (red dots; Online Methods). CD34⁺ cells were transduced with the indicated constructs, starved for 14 h and either left unstimulated (left) or stimulated with 10 ng ml⁻¹ of G-CSF for 15 min (right). Cy3 (red) dots, PLA signals of single proteins or protein–protein complexes; DAPI (blue), nuclei. Representative images are shown. On average, 100 cells were investigated in at least three experiments and evaluated using automated image analysis. Scale bars, 1 μ m. **(e)** CD34⁺ cells of healthy individuals ($n = 3$) were transfected with the indicated constructs and treated or not with G-CSF, and expression of a LEF-1 reporter gene (diagrammed) was measured. Data are mean \pm s.d. derived from three independent experiments, each in triplicate, * $P < 0.05$ compared to cells not treated with G-CSF. RLU, relative light units. **(f)** Fold induction after G-CSF stimulation of LEF-1 and C/EBP α mRNA expression in CD34⁺ cells transduced with indicated constructs. Data are mean \pm s.d. compared to WT HCLS1 and are derived from three independent experiments, each in triplicate, * $P < 0.05$ compared to WT HCLS1. **(g)** CFU assays of CD34⁺ cells from healthy individuals ($n = 3$) transduced with the indicated constructs. Data are mean \pm s.d. derived from three independent experiments, each in duplicate; * $P < 0.05$, ** $P < 0.01$ compared to HCLS1 WT. **(h)** ChIP-re-ChIP assays of nuclear extracts of Jurkat cells to assess HCLS1 binding to LEF-1 at the *LEF1*, *CEBPA* and *CCND1* gene promoters. Antibody to LEF-1 was used in the first ChIP step and antibody to LEF-1 or to HCLS1 for the second ChIP step (Online Methods). Shown is $\Delta\Delta C_i$ of target regions to isotype control (fold enrichment). Data are mean \pm s.d. (derived from two independent experiments).

detected LEF-1–HCLS1 and LEF-1–phospho-HCLS1 complexes in the nuclei of G-CSF-treated CD34⁺ cells transduced with WT HCLS1, but not with HCLS1 NLS or HCLS1 Y397F mutants (Fig. 3c,d). We also found an interaction between endogenous LEF-1 and HAX1 proteins in CD34⁺ cells (data not shown). Similar effects were observed for endogenous HAX1 and phospho-HCLS1 proteins (data not shown). Furthermore, knockdown of HAX1 in CD34⁺ cells prevented the LEF-1–phospho-HCLS1 interaction (data not shown).

Autoregulation of LEF-1 mRNA expression upon binding of LEF-1 protein to its own promoter is well established and is a common feature of many transcription factors. To evaluate the effects of HCLS1 on LEF-1 autoregulation, we generated a reporter gene construct comprising 3.6 kb of the human *LEF1* gene promoter with five LEF-1-binding sites. G-CSF activated the *LEF1* promoter in CD34⁺ cells; transfection of LEF-1 or HCLS1 cDNAs led to further upregulation of G-CSF-dependent *LEF1* promoter activity, with synergistic effects of LEF-1 and HCLS1 (Fig. 3e). However, a LEF-1 cDNA with a mutated HCLS1-binding site (encoding LEF-1 Ala16) did not activate the LEF-1 promoter. HCLS1 Y397F also did not activate the promoter, indicating that phosphorylation of HCLS1 is important for LEF-1 autoregulation. The HCLS1 NLS mutant also did not activate *LEF1* gene promoter. The effects of LEF-1 and HCLS1 on G-CSF-triggered *LEF1* promoter activation in CD34⁺

cells were severely diminished by knockdown of HCLS1 or HAX1 (Supplementary Fig. 10a–c). We observed similar effects on the *CEBPA* gene promoter in CD34⁺ cells (Supplementary Fig. 11a–d). We also observed similar effects in HEK293T cells on the *LEF1* gene promoter and in these cells using the TOP-FOP flash plasmid system, in which the TOP reporter contains six LEF-1- and TCF-binding sites (which are lacking in the FOP reporter) (Supplementary Fig. 12a–c and data not shown).

Consistent with these results, HCLS1 Y397F and HCLS1 NLS mutants did not activate mRNA expression of LEF-1 and LEF-1 target genes in CD34⁺ cells upon G-CSF treatment (Fig. 3f and data not shown). The inhibitory effects of a LEF-1-specific shRNA on C/EBP α mRNA expression in CD34⁺ cells were rescued by LEF-1 or dnLEF-1 cDNAs, but not by the LEF-1 Ala16 mutant cDNA (Supplementary Fig. 12d). In agreement with these findings, cells transduced with LEF-1 Ala16, HCLS1 Y397F or HCLS1 NLS showed reduced granulocyte colony and granulocyte-macrophage colony (CFU-G and CFU-GM) activities compared to control cells or cells transduced with WT LEF-1 or WT HCLS1 (Fig. 3g).

We further analyzed whether HCLS1 activates LEF-1 target genes by binding to LEF-1 on chromatin. We carried out chromatin immunoprecipitation (ChIP) using chromatin from Jurkat cells. Using antibody to LEF-1, we first detected LEF-1 binding to chromatin of LEF-1

target genes (*LEF1*, *CCND1* and *CEBPA*; first ChIP). In a second round, we carried out a re-ChIP experiment using DNA from the first round of ChIP, using antibody to LEF-1 (as positive control) or antibody to HCLS1 (second ChIP). We found that LEF-1 but not HCLS1 binds the LEF-1 target genes tested (Fig. 3h).

Reciprocal feedback regulation of HCLS1 by LEF1

Because HCLS1 mRNA expression is activated by G-CSF in hematopoietic cells of healthy individuals, we analyzed whether LEF-1 could be involved in feedback regulation of HCLS1. In CD34⁺ cells, LEF-1 knockdown resulted in diminished HCLS1 mRNA and protein expression (Supplementary Fig. 13a,b). We identified two LEF-1- and three C/EBP α -binding sites within the 1,600-bp *HCLS1* gene promoter and verified LEF-1 binding to the promoter by ChIP assay in CD34⁺ cells (Supplementary Fig. 13c,d). We also made a reporter gene construct containing 1,600 bp of the *HCLS1* gene promoter and found activation of the *HCLS1* gene promoter by LEF-1 in HEK293T cells (Supplementary Fig. 13e). *HCLS1* promoter activity was induced by LEF-1 in CD34⁺ cells, and G-CSF treatment further enhanced LEF-1-triggered activation of promoter activity (Supplementary Fig. 13f). LEF-1 knockdown or mutation of LEF-1-binding sites within the *HCLS1* gene promoter substantially inhibited G-CSF-dependent activation of the promoter (Supplementary Fig. 13f).

HCLS1 and HAX1 are involved in PI3K-Akt activation by G-CSF

HCLS1 is associated with the PI3K-Akt pathway⁹, and this pathway is known to be activated by G-CSF²⁰. We therefore wanted to determine whether HCLS1 is involved in G-CSF-triggered activation of PI3K-Akt signaling. Microarray analysis revealed substantial inhibition of the PI3K-Akt pathway by HCLS1-specific shRNA compared with control shRNA in CD34⁺ cells (Supplementary Table 3). Treatment

of CD34⁺ cells with G-CSF led to phosphorylation of PI3K p85 (on Tyr458) and of Akt (on Ser473), which were both markedly reduced in cells transduced with HCLS1- or HAX1-specific shRNA (Fig. 4a,b). Similarly, we detected much lower amounts of G-CSF-dependent phospho-PI3K p85 (Tyr458) and phospho-Akt (Ser473) in CD34⁺ cells of patients with congenital neutropenia as compared with cells from healthy individuals (Supplementary Fig. 14a,b). In experiments in which WT HCLS1 or HCLS1 NLS were expressed in CD34⁺ cells, removal of the NLS in HCLS1 did not affect G-CSF-triggered activation of PI3K or Akt (Fig. 4c,d).

HCLS1 and HAX1 control G-CSF-induced F-actin rearrangement

HCLS1 is involved in F-actin rearrangement^{3,9,11,12}, which is impaired in myeloid cells of patients with congenital neutropenia⁴⁷. Microarray analysis showed marked defects in the actin regulatory pathway after HCLS1 knockdown (Supplementary Table 3). We therefore determined whether G-CSF-triggered F-actin rearrangement depends on HCLS1 and/or HAX1. As in patients with congenital neutropenia⁴⁷, basal F-actin amounts were significantly greater in CD34⁺ cells transduced with HAX1- or HCLS1-specific shRNA compared with control shRNA (Fig. 4e and Supplementary Fig. 15a). G-CSF treatment of CD34⁺ cells led to a rapid, transient increase in F-actin content, which was abrogated by HAX1 or HCLS1 knockdown (Fig. 4f and Supplementary Fig. 15b). However, expression of WT HCLS1 or HCLS1 NLS did not affect G-CSF-triggered F-actin rearrangement (Fig. 4g).

To further test the role of HAX1 in F-actin dynamics, we used HEK293T cells, which do not express HCLS1 but express its homolog cortactin, and which also express HAX1. In HEK293T cells transfected with G-CSFR cDNA (293T-G-CSFR cells), we observed a fine, homogenous F-actin structure on the cell membrane and in the

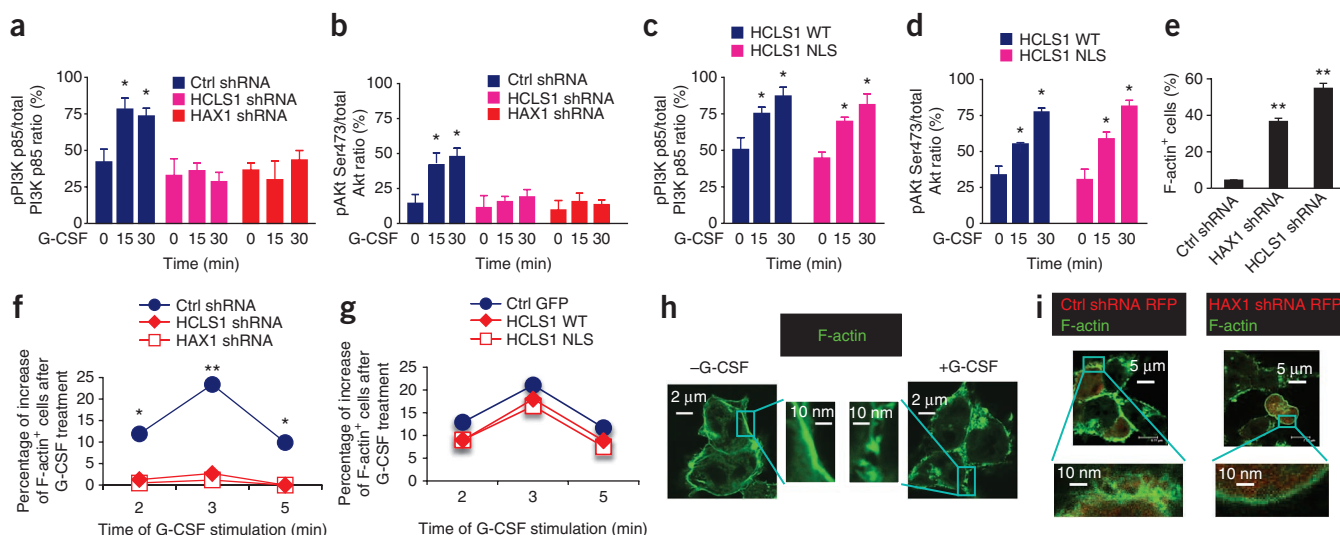
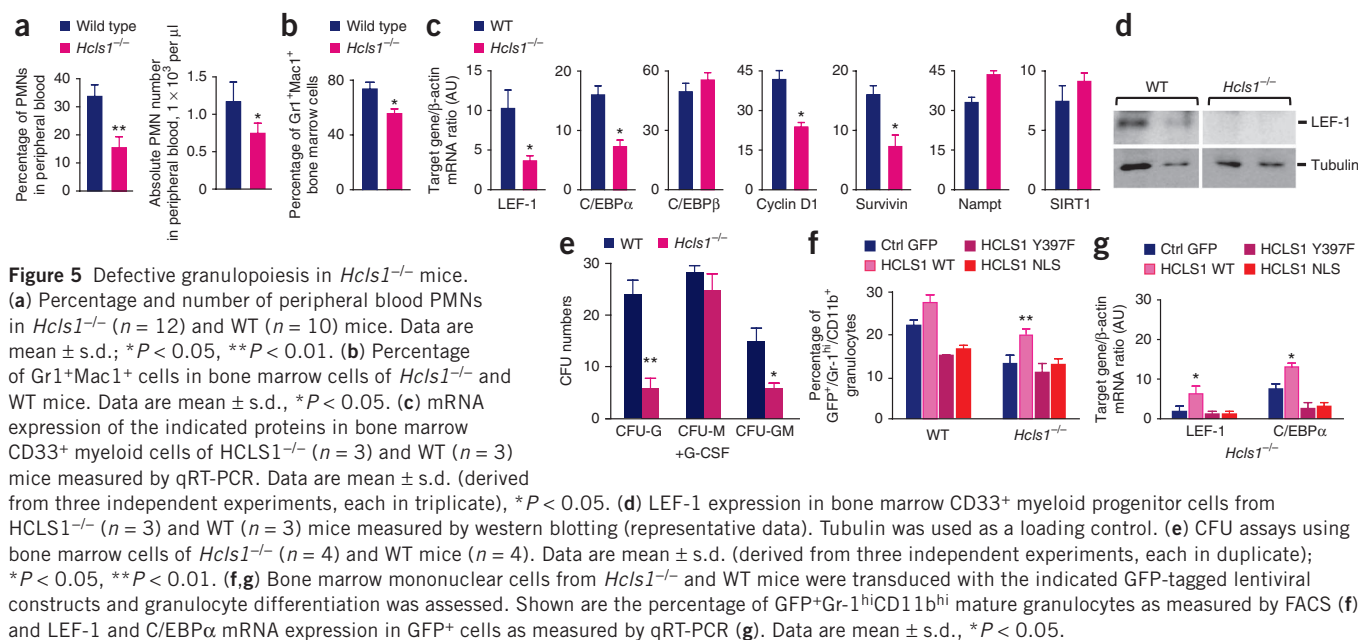


Figure 4 HCLS1 and HAX1 are required for G-CSF-triggered phosphorylation of PI3K p85 and Akt and for F-actin rearrangement. (a–d) CD34⁺ cells of healthy individuals ($n = 3$) were transduced with the indicated constructs, and RFP⁺ or GFP⁺ cells were sorted and treated with 10 ng ml⁻¹ of G-CSF or left untreated. At the indicated time points, the cells were harvested, fixed and permeabilized cells and amounts of total PI3K p85 and phospho-PI3K p85 (Tyr458) (a,c) and total Akt and phospho-Akt (Ser473) (b,d) were quantified using FACS analysis. Shown is the percentage of phospho- to total protein-positive cells. Data are mean \pm s.d. (derived from two independent experiments, each in duplicate), * $P < 0.05$. (e–g) CD34⁺ cells were transduced with the indicated constructs, treated with 10 ng ml⁻¹ of G-CSF for the indicated lengths of time or left untreated, and F-actin staining was assessed by FACS. Shown are the percentage of RFP⁺ cells that are F-actin⁺ (e) and the percentage increase of F-actin⁺ cells after stimulation with G-CSF (f,g). Data are mean \pm s.d. (derived from three independent experiments each in duplicate); * $P < 0.05$, ** $P < 0.01$. (h,i) Representative images showing the distribution of F-actin in HEK293T cells transduced with G-CSFR cDNA (293T-GCSFR) and subsequently treated with 10 ng ml⁻¹ of G-CSF for 3 min or left untreated was assessed by confocal microscopy. In i cells were co-transduced with control or HAX1 shRNA. Insets show higher magnification views.



cytoplasm. This structure was rapidly redistributed after G-CSF treatment (Fig. 4h), and this redistribution was blocked by HAX1 knockdown (Fig. 4i).

Hcls1^{-/-} mice have mild neutropenia

We further evaluated the role of HCLS1 in granulopoiesis *in vivo* using *Hcls1*^{-/-} mice. We found significantly fewer peripheral blood neutrophilic granulocytes in *Hcls1*^{-/-} mice compared with WT mice (Fig. 5a). In addition, *Hcls1*^{-/-} mice had moderately more monocytes and eosinophils, slightly fewer thrombocytes and similar numbers of lymphocytes and erythrocytes compared with WT mice (Supplementary Table 2). Consistent with these results, *Hcls1*^{-/-} mice had fewer Gr1⁺Mac1⁺ cells (Fig. 5b), slightly fewer granulocyte-monocyte progenitors and similar numbers of common myeloid progenitors and megakaryocyte-erythroid progenitors compared with WT littermates (Supplementary Fig. 16). mRNA and protein expression of LEF-1 and mRNA expression of LEF-1 target genes were significantly lower in *Hcls1*^{-/-} CD33⁺ bone marrow myeloid progenitors compared with cells of WT mice (Fig. 5c,d). mRNA levels of Nampt, SIRT1 and C/EBP β , which are involved in emergency granulopoiesis²², were similar or slightly higher in the *Hcls1*^{-/-} cells than in WT cells (Fig. 5c). Bone marrow cells from *Hcls1*^{-/-} mice formed fewer CFU-G and CFU-M colonies, but similar numbers of BFU-E and CFU-Mega colonies, compared to cells from WT mice (Fig. 5e and Supplementary Fig. 17a). *Hcls1*^{-/-} CFU-G colonies had lower expression of LEF-1 and C/EBP α mRNA, but higher expression of NAMPT, C/EBP β and SIRT1 mRNA, compared with WT colonies (Supplementary Fig. 17b). We next carried out a rescue experiment in which we transduced *Hcls1*^{-/-} bone marrow cells with HCLS1 cDNA constructs and assessed *in vitro* granulocytic differentiation using a liquid culture assay. *Hcls1*^{-/-} cells transduced with WT HCLS1 cDNA, but not with the HCLS1 Y397F or HCLS1 NLS cDNAs, showed elevated numbers of Gr-1^{hi}CD11b^{hi} mature granulocytes, comparable to cells from WT mice (Fig. 5f). Consistent with these observations, *Hcls1*^{-/-} cells transduced with WT HCLS1 cDNA had elevated amounts of LEF-1 and C/EBP α mRNA (Fig. 5g).

Elevated levels of HCLS1 in human AML leukemic blasts

The functional outcomes of HCLS1 and LEF-1 action are dose dependent. For example, HCLS1 is hyperactivated in chronic lymphocytic leukemia¹³, and constitutively activated LEF-1 induces AML in mice⁴¹. Therefore, we were interested in determining the level of HCLS1 expression in AML blasts. Compared with CD34⁺ or CD33⁺ cells of healthy individuals, blast cells of patients with AML showed significantly higher expression of HCLS1 mRNA (Supplementary Fig. 18a). Moreover, immunohistochemistry of tissue arrays containing bone marrow biopsies from patients with AML showed significantly higher HCLS1 protein expression in blasts of 46 of 52 (88.46%) patients with AML, as compared with biopsies from healthy individuals (Fig. 6a and Supplementary Table 3). Using Duolink PLA, we found that HCLS1 protein interacted with LEF-1 protein in primary AML blasts (data not shown). HCLS1 or LEF-1 knockdown in blasts of three patients with AML led to significantly lower cell proliferation and greater apoptosis, in agreement with lower mRNA expression of LEF-1 target genes (Fig. 6b, Supplementary Fig. 18b and data not shown). Because HCLS1 is activated by G-CSF, we measured G-CSF expression in AML blasts and found substantial synthesis of G-CSF by these cells in three out of five patients, as compared with CD34⁺ hematopoietic or CD33⁺ myeloid progenitor cells of healthy individuals (Fig. 6c). As not all of the patients with AML that we tested have G-CSF-producing leukemic cells, we carried out a meta-analysis of publicly available microarray data and found substantial mRNA upregulation of hematopoietic cytokines (G-CSF, TPO, SCF and EPO) and/or their receptors in AML blasts (Supplementary Table 4). Therefore, autocrine production of G-CSF or other cytokines by AML blasts might underlie elevated HCLS1 expression.

Activating insertion in exon 12 of HCLS1 in patients with AML

To evaluate whether genetic abnormalities are responsible for elevated HCLS1 levels in patients with AML, we sequenced exons of the *HCLS1* gene in such patients. We found a 12-bp insertion (1153insCCCGAGCCTGAG, NM_005335; Pro-Glu-Pro-Glu 366-367ins) in exon 12 of the *HCLS1* gene, which encodes the proline-rich domain, in 89 of 135 patients with AML (65.9%) and in 41 of 104 healthy individuals (39.4%) (Fig. 6d; Supplementary Table 5).

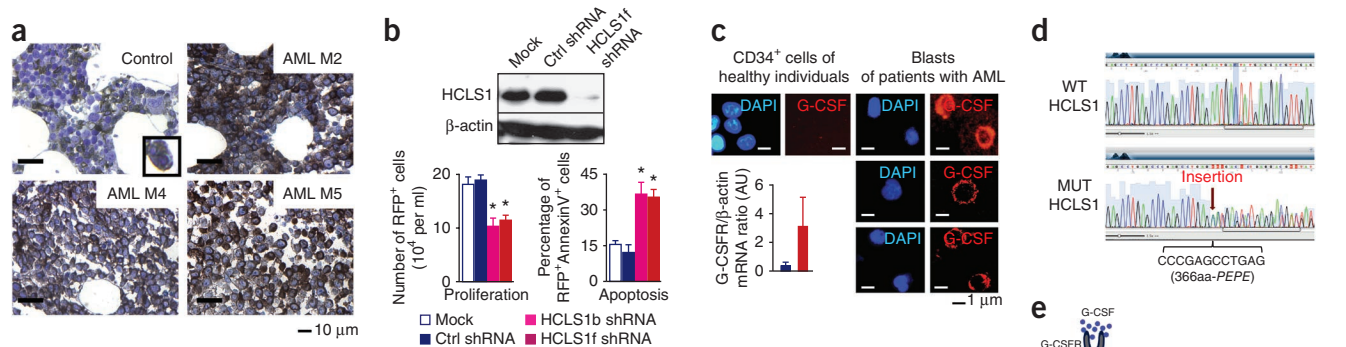


Figure 6 HCLS1 is hyperactivated in AML. **(a)** Representative micrographs of immunohistochemistry of HCLS1 (brown) counterstained with hematoxylin (blue) of bone marrow sections of one healthy individual (control) and three patients with AML with different AML types (AML M2, M4 and M5). **(b)** Primary blasts of three patients with AML were transfected with control-RFP shRNA or either of two HCLS1-RFP shRNAs. RFP⁺ cells were sorted and used for further experiments. Top, representative western blot showing HCLS1 expression; β -actin was used as a loading control. Bottom, on day 7 cell proliferation was assessed by counting of viable RFP⁺ cells and apoptosis was assessed by annexin V staining of RFP⁺ cells. Data are mean \pm s.d. (derived from three independent experiments, each in triplicate), * $P < 0.05$. **(c)** Representative images of intracellular staining of G-CSF in CD34⁺ cells of healthy individuals ($n = 3$) and in blasts of three patients with AML were measured using the Duolink *in situ* PLA assay with antibody to G-CSF. Nuclear DAPI staining (blue) and G-CSF staining (red). Inset, G-CSFR mRNA expression in AML blasts (red bar, $n = 3$) and in CD34⁺ cells of healthy individuals (blue bar, $n = 3$). Data are mean \pm s.d. (derived from three independent experiments, each in triplicate). **(d)** Representative images of Sanger DNA sequencing of the *HCLS1* gene from one healthy individual with WT HCLS1 and one patient with AML with the 12-bp insertion (MUT HCLS1). **(e)** Model of the interplay among HCLS1, HAX1 and LEF-1. Activation of G-CSF receptor leads to phosphorylation and activation of HCLS1 via Lyn and Syk. HCLS1 together with HAX1 binds LEF-1, transporting LEF-1 into the nucleus, where LEF-1 activates target genes (for example, *LEF1*, *CEBPA* and *HCLS1*) and promotes granulocytic differentiation.

The percentage of patients with AML with heterozygous or homozygous HCLS1 Pro-Glu-Pro-Glu 366-367ins was significantly higher compared to that of healthy individuals (odds ratios 2.31 and 1.64, respectively; $P = 0.0001389$). The allele frequency of HCLS1 Glu-Pro-Glu-Pro366-367ins was also significantly higher in patients with AML as compared with healthy individuals (35.2% versus 21.5%, odds ratio 1.7; $P = 0.0005313$). Notably, the high frequency of this insertion was previously described in patients with systemic lupus erythematosus and HCLS1 containing the inserted amino acids was shown to enhance B cell receptor signaling in B lymphocytes, inducing receptor-independent activation⁴⁸. Similar mechanisms of HCLS1 hyperactivation could be applicable to AML blasts.

DISCUSSION

We identified HCLS1 to be crucial in at least three G-CSFR signaling pathways, connecting G-CSFR signaling with LEF-1 and with the PI3K-Akt and F-actin pathways (Fig. 6e). Notably, interaction of HCLS1 with LEF-1 is essential for myeloid differentiation. The tyrosine kinases Lyn and Syk are essential for G-CSFR signaling in myeloid cells^{15,16,23,24}, and HCLS1 is a major substrate of Lyn and Syk^{3,5-7}. We found that in myeloid cells Syk is constitutively associated with HCLS1, and upon G-CSF stimulation HCLS1 is tyrosine-phosphorylated and complexed with Lyn. The functional importance of HCLS1 for G-CSF-induced granulopoiesis is supported by the observation that G-CSF-triggered myeloid differentiation of CD34⁺ cells is substantially impaired after knockdown of HCLS1 or its binding partner HAX1. Patients with congenital neutropenia, who have disrupted G-CSFR-triggered granulopoiesis, have mutations in *HAX1*, leading to a lack of HAX1 protein²⁹. In these patients, G-CSF did not activate HCLS1 and LEF-1. Similarly, *Hcls1*^{-/-} mice have mild neutropenia and lower expression of LEF-1 in myeloid cells compared with WT mice.

Because HAX1 is a ubiquitously expressed protein³⁰⁻³³, it has been unclear why patients with congenital neutropenia have isolated

neutropenia only. We found that in such patients with *HAX1* mutations, G-CSF did not induce expression and function of the hematopoietic-specific HAX1-binding partner HCLS1. Therefore, we suggest that both HAX1 and HCLS1 are required for G-CSFR signaling and that downregulation of HCLS1 expression and functions causes isolated myeloid defects in patients with congenital neutropenia.

What is the mechanism of maturation arrest of granulopoiesis in patients with congenital neutropenia? We previously showed that LEF-1 is essential for granulocytic differentiation via binding to *C/EBP α* and that a lack of both LEF-1 and *C/EBP α* in myeloid progenitors from patients with congenital neutropenia caused maturation arrest of granulopoiesis³⁴. However, the mechanisms by which LEF-1 is activated upon G-CSF stimulation and by which LEF-1 is downregulated in patients with congenital neutropenia downstream of HAX1 mutations have been unclear. In the search for a hematopoietic-specific binding partner of LEF-1, we found an interaction between the HCLS1 and LEF-1 proteins. This interaction is indispensable for G-CSF-dependent proliferation and differentiation of myeloid cells.

After tyrosine phosphorylation, HCLS1 translocates to the nucleus via its NLS². B cell receptor (BCR) cross-linking causes nuclear translocation of tyrosine-phosphorylated HCLS1 that is mediated by Lyn and Syk⁷. We found that in CD34⁺ cells, HCLS1 interacts with LEF-1 and upon G-CSF stimulation is phosphorylated and translocates together with LEF-1 into the nucleus. Moreover, LEF-1 with a mutated HCLS1-binding site could not migrate to the nucleus, and LEF-1 was not found in the nucleus in the presence of HCLS1 lacking its NLS. This HCLS1 mutant did not activate the *LEF1* gene promoter or induce LEF-1 mRNA expression, did not promote CFU-G colony formation and did not rescue defective granulopoiesis in *Hcls1*^{-/-} bone marrow cells *in vitro*, similarly to an HCLS1 mutant lacking the Y397 phosphorylation site. LEF-1 also has an NLS, and it has been assumed that LEF-1 translocates into the nucleus via the classical

nuclear import pathway through binding of the LEF-1 NLS to importins (refs. 49,50). However, recent studies have shown that the nuclear transport of LEF-1 is mediated by at least two independent pathways, one that depends on the NLS of LEF-1 and another that depends on LEF-1-binding partners. For example, β -catenin-dependent nuclear translocation of LEF-1 is independent of the LEF-1 NLS⁵¹. LEF-1 is a key protein in the Wnt signaling cascade, and the intracellular localization of LEF-1 varies depending on cell type and differentiation stage in order to regulate Wnt signaling appropriately. For example, in neurons and ectodermal cells LEF-1 is largely localized in the cytoplasm, whereas in astrocytes and mesodermal cells LEF-1 accumulates in the nucleus^{52,53}. In our study, we demonstrated the indispensable role of HCLS1 in nuclear transport of LEF-1 in CD34⁺ cells upon G-CSF-triggered myeloid differentiation, which is independent of the LEF-1 NLS. This nuclear transport also seems to be independent of β -catenin, given the similar behavior of dnLEF-1, which does not bind to β -catenin. Similarly to aspects of our model, LEF-1 directs the differentiation of keratinocyte stem cells along the hair follicle lineage via an interaction with the vitamin D receptor that is independent of β -catenin⁵⁴. HCLS1 has not been reported to bind DNA or to be present on chromatin, and we did not detect HCLS1 associated with LEF-1 on chromatin of LEF-1 target genes. These results therefore indicate that HCLS1 is involved in the transport of LEF-1 into the nucleus but not in LEF-1 binding and activation of its target genes.

In addition to activating HCLS1 by phosphorylation, G-CSF induced mRNA and protein expression of HCLS1. The *HCLS1* gene promoter has binding sites for the myeloid-specific transcription factors LEF-1 and C/EBP α , and LEF-1 activated HCLS1 expression by direct binding to the *HCLS1* gene promoter. These data indicate the existence of a feedback loop by which G-CSF and LEF-1 promote HCLS1 expression, which in turn promotes LEF-1 function.

HAX1 is constitutively associated with HCLS1³⁰, and we found that HAX1 is present in a complex with HCLS1 and LEF-1 and is essential for the HCLS1-LEF-1 interaction. These results may help explain how *HAX1* mutations lead to isolated neutropenia in patients with congenital neutropenia.

An absence of HAX1 or HCLS1 in CD34⁺ cells led to abrogation of G-CSF-triggered activation of PI3K and Akt. Similarly, CD34⁺ cells from patients with congenital neutropenia with *HAX1* mutations showed only marginal G-CSF-triggered activation of these proteins. Expression of HCLS1 lacking its NLS could not induce granulocytic differentiation or activate LEF-1 and had no effects on PI3K-Akt signaling. We therefore propose that both the Wnt-LEF-1 and PI3K-Akt pathways are involved in hematopoietic cell proliferation and granulocytic differentiation and that they act independently of each other. Microarray analysis of CD34⁺ cells deficient in HCLS1 protein showed downregulation of components of multiple signaling systems other than Wnt and PI3K-Akt. For instance, *MDM2* was among the most down-regulated genes, which regulates cell fate decision via its interaction with Numb⁵⁵. HCLS1 has broad effects on hematopoietic cell proliferation and differentiation, and further functional studies are required.

HCLS1 is essential for G-CSFR-dependent F-actin rearrangement. HCLS1 contains F-actin-binding domains, which interact with actin filaments and regulate their assembly^{3,9,11,12}. In T and B lymphocytes, actin dynamics are controlled by tyrosine-phosphorylated HCLS1 in a complex with WASP and Arp2-Arp3. We previously showed that basal F-actin content in myeloid cells of patients with congenital neutropenia is greater than in cells of normal individuals, but that the increase in F-actin expression after G-CSF treatment is significantly lower compared to normal cells⁴⁷. Consistent with those results, knockdown of

HCLS1 or HAX1 in CD34⁺ cells of healthy individuals led to an increase in F-actin expression, which was not further elevated by G-CSF. Disturbed F-actin reorganization may lead to defective polarization and/or migration of hematopoietic cells within the bone marrow niche, which is essential for their differentiation⁵⁶. F-actin might also function as a scaffold protein in G-CSFR signaling (for example, by acting as a scaffold for LEF-1).

HCLS1 may be involved in AML pathogenesis, as HCLS1 protein expression was substantially elevated in blasts of patients with AML as compared to bone marrow cells from healthy individuals. AML blasts respond hyperactively to hematopoietic cytokines such as G-CSF, GM-CSF, IL-3 and TPO, and also have greater levels of total protein tyrosine phosphorylation⁵⁷. Autocrine production of hematopoietic cytokines such as GM-CSF, G-CSF, M-CSF and IL-6 by AML blasts has been reported⁵⁸⁻⁶⁰. In accordance with these data, we found extremely high autocrine production of G-CSF by AML blasts. High expression of G-CSF or other hematopoietic cytokines in AML blasts and the action of such cytokines in an autocrine or paracrine manner may induce hyperactivation of HCLS1 and lead to uncontrolled cell proliferation and reduced apoptosis. Indeed, in a meta-analysis of microarray data from patients with AML, we identified patients expressing high amounts of G-CSF, TPO or EPO or their receptors. The finding that hyperactivation of HCLS1 protein is involved in leukemic cell proliferation is also supported by data from patients with chronic lymphoblastic leukemia with poor prognosis; in these patients, HCLS1 is hyperphosphorylated owing to stimulation triggered by a persistent BCR-mediated Syk phosphorylation¹³. Moreover, we identified an insertion in the proline-rich region of HCLS1 in a majority of patients with AML. This insertion was previously identified in a mouse immature B lymphoma cell line in which it induced enhanced BCR-mediated signal transduction⁴⁸. In AML, this insertion may lead to hyperactivation of cytokine signaling.

In summary, both HAX1 and HCLS1 are essential for multiple aspects of G-CSFR signaling pathways involving LEF-1, PI3K-Akt and F-actin and are essential for granulopoiesis. Our data suggest a dose-dependent function of HCLS1 in myeloid cell proliferation and differentiation: in congenital neutropenia HCLS1 is markedly down-regulated and myelopoiesis is abrogated, whereas in AML HCLS1 is hyperactivated and associated with the high proliferative capacity of leukemic cells. We and others have described similar phenomena for LEF-1: in the absence of LEF-1, myeloid differentiation of human hematopoietic stem cells is markedly diminished³⁴, and in a mouse model, constitutive hyperactivation of LEF-1 leads to hyperproliferative responses of hematopoietic cells with subsequent transformation into AML⁴¹.

METHODS

Methods and any associated references are available in the online version of the paper.

Accession codes. Microarray data have been deposited in the Gene Expression Omnibus (GEO) database with accession code GSE40712.

Note: Supplementary information is available in the online version of the paper.

ACKNOWLEDGMENTS

We thank A. Gigina, K. Cherkaoui, A. Müller Brechlin, M. Reuter and A.-L. Hagemann for technical assistance. We thank J. Klupp for assistance in generation of LEF-1 Ala16 mutant; D.D. Billadeau (Department of Immunology, Schulze Center for Novel Therapeutics, College of Medicine, Mayo Clinic) for providing us with the rabbit polyclonal HCLS1-specific antibody; L. Naldini (San Raffaele Telethon Institute for Gene Therapy, Division of Regenerative Medicine, Gene Therapy and

Stem Cells, San Raffaele Institute) for pRRL.PPT.PGK.GFPpre vector; A. Schambach (Department of Experimental Hematology, Hannover Medical School) for VSVg envelope plasmid; Thomas J. Hope (University of Illinois at Chicago) for pRSV-Rev plasmid; and O. Tetsu (Department of Otolaryngology—Head and Neck Surgery, University of California—San Francisco) for the *CCND1* reporter construct. We also thank the physicians within the Severe Chronic Neutropenia International Registry for providing patient material. We thank study subjects for their cooperation. This work was partially supported by German José Carreras Leukemia Foundation (J.S., M.K.), by REBIRTH Cluster of Excellence of the Hannover Medical School (J.S.), by Madeleine Schickedanz-KinderKrebs-Stiftung (J.S.), and by the Deutsche Forschungsgemeinschaft (Z.L.; DFG grant Li 1608/2-1).

AUTHOR CONTRIBUTIONS

K.W. and J.S. made initial observations, designed the experiments, analyzed the data, supervised experimentation and wrote the manuscript; J.S., D.L., M.K., O.K., A.G. and I.K. performed the main experiments; K.G. introduced mutations into LEF-1 and C/EBP α reporter gene constructs and performed reporter gene assays in HEK293T cells; J.B. and E.C. performed blood cell counting in *Hcls1*^{-/-} mice and provided bone marrow and blood material of these mice; K.H. and H.-H.K. performed tissue microarray analysis; Z.L. and A.G. provided some of the AML samples; C.S. and R.G. introduced mutations in LEF-1 cDNA corresponding to HCLS1-binding site; C.Z. provided patient material.

COMPETING FINANCIAL INTERESTS

The authors declare no competing financial interests.

Published online at <http://www.nature.com/doi/10.1038/nm.2958>.

Reprints and permissions information is available online at <http://www.nature.com/reprints/index.html>.

- Kitamura, D., Kaneko, H., Miyagoe, Y., Ariyasu, T. & Watanabe, T. Isolation and characterization of a novel human gene expressed specifically in the cells of hematopoietic lineage. *Nucleic Acids Res.* **17**, 9367–9379 (1989).
- van Rossum, A.G., Schuurin-Scholtes, E., van Buuren-van Seggelen, V., Kluin, P.M. & Schuurin, E. Comparative genome analysis of cactortin and HS1: the significance of the F-actin binding repeat domain. *BMC Genomics* **6**, 15 (2005).
- Huang, Y. & Burkhardt, J.K. T-cell-receptor-dependent actin regulatory mechanisms. *J. Cell Sci. Review* **120**, 723–730 (2007).
- Hao, J.J., Carey, G.B. & Zhan, X. Syk-mediated tyrosine phosphorylation is required for the association of hematopoietic lineage cell-specific protein 1 with lipid rafts and B cell antigen receptor signalosome complex. *J. Biol. Chem.* **279**, 33413–33420 (2004).
- Takemoto, Y. *et al.* Growth factor receptor-bound protein 2 (Grb2) association with hematopoietic specific protein 1: linkage between Lck and Grb2. *J. Immunol.* **161**, 625–630 (1998).
- Ingle, E. *et al.* HS1 interacts with Lyn and is critical for erythropoietin-induced differentiation of erythroid cells. *J. Biol. Chem.* **275**, 7887–7893 (2000).
- Yamanashi, Y. *et al.* Identification of HS1 protein as a major substrate of protein-tyrosine kinase(s) upon B-cell antigen receptor-mediated signaling. *Proc. Natl. Acad. Sci. USA* **90**, 3631–3635 (1993).
- Brunati, A.M. *et al.* Thrombin-induced tyrosine phosphorylation of HS1 in human platelets is sequentially catalyzed by Syk and Lyn tyrosine kinases and associated with the cellular migration of the protein. *J. Biol. Chem.* **280**, 21029–21035 (2005).
- Kahner, B.N. *et al.* Hematopoietic lineage cell-specific protein 1 (HS1) is a functionally important signaling molecule in platelet activation. *Blood*. **110**, 2449–2456 (2007).
- Yamanashi, Y. *et al.* Role of tyrosine phosphorylation of HS1 in B cell antigen receptor-mediated apoptosis. *J. Exp. Med.* **185**, 1387–1392 (1997).
- Uruno, T., Zhang, P., Liu, J., Hao, J.J. & Zhan, X. Haematopoietic lineage cell-specific protein 1 (HS1) promotes actin-related protein (Arp) 2/3 complex-mediated actin polymerization. *Biochem. J.* **371**, 485–493 (2003).
- Huang, Y. *et al.* The c-Abl tyrosine kinase regulates actin remodeling at the immune synapse. *Blood* **112**, 111–119 (2008).
- Scielzo, C. *et al.* HS1 protein is differentially expressed in chronic lymphocytic leukemia patient subsets with good or poor prognoses. *J. Clin. Invest.* **115**, 1644–1650 (2005).
- Taniuchi, I. *et al.* Antigen-receptor induced clonal expansion and deletion of lymphocytes are impaired in mice lacking HS1 protein, a substrate of the antigen-receptor-coupled tyrosine kinases. *EMBO J.* **14**, 3664–3678 (1995).
- Corey, S.J. *et al.* Requirement of Src kinase Lyn for induction of DNA synthesis by granulocyte colony-stimulating factor. *J. Biol. Chem.* **273**, 3230–3235 (1998).
- Corey, S.J. & Anderson, S.M. Src-related protein tyrosine kinases in hematopoiesis. *Blood Review* **93**, 1–14 (1999).
- Ward, A.C., Monkhouse, J.L., Hamilton, J.A. & Csar, X.F. Direct binding of Shc, Grb2, SHP-2 and p40 to the murine granulocyte colony-stimulating factor receptor. *Biochim. Biophys. Acta* **1448**, 70–76 (1998).
- Ward, A.C. *et al.* Tyrosine-dependent and -independent mechanisms of STAT3 activation by the human granulocyte colony-stimulating factor (G-CSF) receptor are differentially utilized depending on G-CSF concentration. *Blood* **93**, 113–124 (1999).
- Zhu, Q.S., Robinson, L.J., Roginskaya, V. & Corey, S.J. G-CSF-induced tyrosine phosphorylation of Gab2 is Lyn kinase dependent and associated with enhanced Akt and differentiative, not proliferative, responses. *Blood* **103**, 3305–3312 (2004).
- Zhu, Q.S. *et al.* G-CSF induced reactive oxygen species involves Lyn-P13-kinase-Akt and contributes to myeloid cell growth. *Blood* **107**, 1847–1856 (2006).
- Kendrick, T.S. & Bogoyevitch, M.A. Activation of mitogen-activated protein kinase pathways by the granulocyte colony-stimulating factor receptor: mechanisms and functional consequences. *Front. Biosci. Review* **12**, 591–607 (2007).
- Skokowa, J. *et al.* NAMPT is essential for the G-CSF-induced myeloid differentiation via a NAD⁺-sirtuin-1-dependent pathway. *Nat. Med.* **15**, 151–158 (2009).
- Akbarzadeh, S. *et al.* Tyrosine residues of the granulocyte colony-stimulating factor receptor transmit proliferation and differentiation signals in murine bone marrow cells. *Blood* **99**, 879–887 (2002).
- Corey, S.J. *et al.* Granulocyte colony-stimulating factor receptor signaling involves the formation of a three-component complex with Lyn and Syk protein-tyrosine kinases. *Proc. Natl. Acad. Sci. USA* **91**, 4683–4687 (1994).
- Ward, A.C. *et al.* The SH2 domain-containing protein tyrosine phosphatase SHP-1 is induced by granulocyte colony-stimulating factor (G-CSF) and modulates signaling from the G-CSF receptor. *Leukemia* **14**, 1284–1291 (2000).
- Basu, S., Dunn, A. & Ward, A. G-CSF function and modes of action. *Int. J. Mol. Med.* **10**, 3–10 (2002).
- Welte, K., Zeidler, C. & Dale, D.C. Severe congenital neutropenia. *Semin. Hematol.* **43**, 189–195 (2006).
- Zeidler, C., Germeshausen, M., Klein, C. & Welte, K. Clinical implications of ELA2-, HAX1-, and G-CSF-receptor (CSF3R) mutations in severe congenital neutropenia. *Br. J. Haematol.* **144**, 459–467 (2009).
- Klein, C. *et al.* HAX1 deficiency causes autosomal recessive severe congenital neutropenia (Kostmann disease). *Nat. Genet.* **39**, 86–92 (2007).
- Suzuki, Y. *et al.* HAX-1, a novel intracellular protein, localized on mitochondria, directly associates with HS1, a substrate of Src family tyrosine kinases. *J. Immunol.* **158**, 2736–2744 (1997).
- Chao, J.R. *et al.* Hax1-mediated processing of Htra2 by Parl allows survival of lymphocytes and neurons. *Nature* **452**, 98–102 (2002).
- Vafiadaki, E. *et al.* The anti-apoptotic protein HAX-1 interacts with SERCA2 and regulates its protein levels to promote cell survival. *Mol. Biol. Cell* **20**, 306–318 (2009).
- Al-Maghrebi, M. *et al.* The 3' untranslated region of human vimentin mRNA interacts with protein complexes containing eEF-1 γ and HAX-1. *Nucleic Acids Res.* **30**, 5017–5028 (2002).
- Skokowa, J. *et al.* LEF-1 is crucial for neutrophil granulocytopoiesis and its expression is severely reduced in congenital neutropenia. *Nat. Med.* **12**, 1191–1197 (2006).
- Elsner, J., Roesler, J., Emmendorffer, A., Lohmann-Matthes, M.L. & Welte, K. Abnormal regulation in the signal transduction in neutrophils from patients with severe congenital neutropenia: relation of impaired mobilization of cytosolic free calcium to altered chemotaxis, superoxide anion generation and F-actin content. *Exp. Hematol.* **21**, 38–46 (1993).
- Eastman, Q. & Grosschedl, R. Regulation of LEF-1/TCF transcription factors by Wnt and other signals. *Curr. Opin. Cell Biol.* **11**, 233–240 (1999).
- Timm, A. & Grosschedl, R. Wnt signaling in lymphopoiesis. *Curr. Top. Microbiol. Immunol. Review* **290**, 225–252 (2005).
- Bruhn, L., Munnerlyn, A. & Grosschedl, R. ALY, a context-dependent coactivator of LEF-1 and AML-1, is required for TCR α enhancer function. *Genes Dev.* **11**, 640–653 (1997).
- Vadlamudi, U. *et al.* PITX2, β -catenin and LEF-1 interact to synergistically regulate the LEF-1 promoter. *J. Cell Sci.* **118**, 1129–1137 (2005).
- Levanon, D. *et al.* Transcriptional repression by AML1 and LEF-1 is mediated by the TLE/Groucho corepressors. *Proc. Natl. Acad. Sci. USA* **95**, 11590–11595 (1998).
- Petropoulos, K. *et al.* A novel role for Lef-1, a central transcription mediator of Wnt signaling, in leukemogenesis. *J. Exp. Med.* **205**, 515–522 (2008).
- Yaffe, M.B. *et al.* A motif-based profile scanning approach for genome-wide prediction of signaling pathways. *Nat. Biotechnol.* **19**, 348–353 (2001).
- Songyang, Z. *et al.* Use of an oriented peptide library to determine the optimal substrates of protein kinases. *Curr. Biol.* **4**, 973–982 (1994).
- Söderberg, O. *et al.* Direct observation of individual endogenous protein complexes *in situ* by proximity ligation. *Nat. Methods* **3**, 995–1000 (2006).
- Nilsson, I. *et al.* VEGF receptor 2/3 heterodimers detected *in situ* by proximity ligation on angiogenic sprouts. *EMBO J.* **29**, 1377–1388 (2010).
- Greenberg, J.I. *et al.* A role for VEGF as a negative regulator of pericyte function and vessel maturation. *Nature* **456**, 809–813 (2008).
- Elsner, J., Roesler, J., Emmendorffer, A., Lohmann-Matthes, M.L. & Welte, K. Abnormal regulation in the signal transduction in neutrophils from patients with severe congenital neutropenia: relation of impaired mobilization of cytosolic free calcium to altered chemotaxis, superoxide anion generation and F-actin content. *Exp. Hematol.* **21**, 38–46 (1993).
- Otsuka, J. *et al.* Association of a four-amino acid residue insertion polymorphism of the *HS1* gene with systemic lupus erythematosus: molecular and functional analysis. *Arthritis Rheum.* **50**, 871–881 (2004).
- Prieve, M.G., Guttridge, K.L., Munguia, J. & Waterman, M.L. Differential importin- α recognition and nuclear transport by nuclear localization signals within the high-mobility-group DNA binding domains of lymphoid enhancer factor 1 and T-cell factor 1. *Mol. Cell. Biol.* **18**, 4819–4832 (1998).

50. Prieve, M.G., Guttridge, K.L., Munguia, J.E. & Waterman, M.L. The nuclear localization signal of lymphoid enhancer factor-1 is recognized by two differentially expressed Srp1-nuclear localization sequence receptor. *J. Biol. Chem.* **271**, 7654–7658 (1996).
51. Asally, M. & Yoneda, Y. β -catenin can act as a nuclear import receptor for its partner transcription factor, lymphocyte enhancer factor-1 (lef-1). *Exp. Cell Res.* **308**, 357–363 (2005).
52. Coyle-Rink, J., Del Valle, L., Sweet, T., Khalili, K. & Amini, S. Developmental expression of Wnt signaling factors in mouse brain. *Cancer Biol. Ther.* **1**, 640–645 (2002).
53. Arsenian, S., Weinhold, B., Oelgeschläger, M., Rütter, U. & Nordheim, A. Serum response factor is essential for mesoderm formation during mouse embryogenesis. *EMBO J.* **17**, 6289–6299 (1998).
54. Luderer, H.F., Gori, F. & Demay, M.B. Lymphoid enhancer-binding factor-1 (LEF1) interacts with the DNA-binding domain of the vitamin D receptor. *J. Biol. Chem.* **286**, 18444–18451 (2011).
55. Colaluca, I.N. *et al.* Numb controls p53 tumour suppressor activity. *Nature* **451**, 76–80 (2008).
56. Fonseca, A.V., Freund, D., Bornhäuser, M. & Corbeil, D. Polarization and migration of hematopoietic stem and progenitor cells rely on the RhoA/ROCK I pathway and an active reorganization of the microtubule network. *J. Biol. Chem.* **285**, 31661–31671 (2010).
57. Hagiwara, S. *et al.* Tyrosine phosphorylation of proteins in primary human myeloid leukemia cells stimulated by cytokines: analysis of the frequency of phosphorylation, and partial identification and semi-quantification of signaling molecules. *Int. J. Hematol.* **68**, 387–401 (1998).
58. Young, D.C., Wagner, K. & Griffin, J.D. Constitutive expression of the granulocyte-macrophage colony-stimulating factor gene in acute myeloblastic leukemia. *J. Clin. Invest.* **79**, 100–106 (1987).
59. Young, D.C., Demetri, G.D., Ernst, T.J., Cannistra, S.A. & Griffin, J.D. *In vitro* expression of colony-stimulating factor genes by human acute myeloblastic leukemia cells. *Exp. Hematol.* **16**, 378–382 (1988).
60. Ernst, T.J., Ritchie, A.R., O'Rourke, R. & Griffin, J.D. Colony-stimulating factor gene expression in human acute myeloblastic leukemia cells is posttranscriptionally regulated. *Leukemia* **3**, 620–625 (1989).

ONLINE METHODS

Affected and control subjects. Participants in this study included eight patients with severe congenital neutropenia harboring *HAX1* mutations, three patients with neutropenia associated with congenital disorders of metabolism (one patient with glycogen storage disease type Ib and two patients with Shwachman-Diamond syndrome) and two with idiopathic neutropenia. All these subjects had received long-term (>1 year) G-CSF treatment; G-CSF doses ranged between 1.2 and 7.5 mg per kg body weight per day, or every 2 d. Two of the subjects with congenital neutropenia were examined twice, first before initiation of G-CSF therapy and second during long-term G-CSF treatment. Three healthy volunteers received G-CSF at a dose of 5 µg per kg body weight per day for 3 d. We collected bone marrow samples in association with the annual follow-up recommended by the Severe Chronic Neutropenia International Registry. Blood or bone marrow of 135 patients with AML (males and females) and 104 healthy individuals (males and females) were used for sequencing of the *HCLS1* gene. Informed consent was obtained from all subjects. We obtained approval for this study from the Hannover Medical School Institutional Review Board.

Cell purification and separation. We isolated bone marrow and peripheral blood mononuclear cells by Ficoll-Hypaque gradient centrifugation (Amersham Biosciences) and positively selected bone marrow CD34⁺ and CD33⁺ cells by sequential immunomagnetic labeling with corresponding MACS beads (Miltenyi Biotec). Cells were counted, and viability was assessed by Trypan blue dye exclusion. Purity of sorted CD34⁺ and CD33⁺ cells was >96%, as assessed by FACS analysis and by staining with May-Grünwald-Giemsa.

Quantitative real-time RT-PCR. For qRT-PCR, we isolated RNA using Qiagen RNeasy Mini Kit (Qiagen) or TRIZOL reagent (Invitrogen) using the manufacturer's protocol, amplified cDNA using random hexamer primer (Fermentas) and measured mRNA expression using the SYBR Green qRT-PCR kit (Qiagen). Target gene mRNA expression was normalized to β-actin and was represented as arbitrary units. Primer sequences are available upon request.

Western blot analysis. We used the following antibodies: rabbit polyclonal antibody to HCLS1 (1:1,000, J.B. and D.D. Billadeau), rabbit polyclonal antibody to HCLS1 (1:400, Cell Signaling Technology, 4503S), mouse monoclonal antibody to HCLS1 (1:500, BD Bioscience, 610541), rabbit polyclonal antibody to phospho-HCLS1 (Tyr397; 1:100, Cell Signaling Technology, 4507S), rabbit monoclonal antibody to LEF-1 (1:500, Cell Signaling Technology, 22305), mouse monoclonal antibody to LEF-1 (1:1,000, CalBiochem, NA64), mouse monoclonal antibody to Lyn (1:200, Santa Cruz Biotechnology, SC-7274), mouse monoclonal antibody to Syk (1:400, Biologend, 626201), rabbit polyclonal antibody to HAX1 (Santa Cruz Biotechnology, SC-28268), rabbit polyclonal antibody to HA tag (1:1,000, Santa Cruz Biotechnology, SC-2365), mouse monoclonal antibody to β-actin (1:1,000, Santa Cruz Biotechnology, SC-47778) and secondary bovine anti-mouse or goat anti-rabbit HRP-conjugated antibody (1:5,000, Santa Cruz Biotechnology, SC-2371 and SC-2004, respectively). We obtained whole-cell lysates either through lysis of a defined number of cells in RIPA lysis buffer or through direct disruption in Laemmli's loading buffer followed by brief sonication. Cytoplasmic and nuclear cell extracts were isolated using the NE-PER kit (Thermo Scientific). We separated proteins by 10% SDS-PAGE and probed the blots with primary antibody either for 1 h at room temperature or overnight at 4 °C followed by washing.

Two-dimensional blue native/SDS gel electrophoresis of complexes from cell lysates. *Preparation of cell lysates.* Jurkat cells (1×10^7) were harvested and the cell pellet was centrifuged at 350g for 5 min at 4 °C. The cell pellet was washed three times with ice-cold PBS, resuspended in 250 µl ice-cold BN-lysis buffer (20 mM Bis-tris, 500 mM ε-aminocaproic acid, 20 mM NaCl, 2 mM EDTA, pH 8.0, 10% glycerol, pH to 7.0 with HCl, 1% digitonin, Halt protease inhibitor cocktail from Pierce), incubated on ice for 15 min and centrifuged at 13,000g for 15 min at 4 °C to remove cell debris. Cell lysate (100–150 µl) was dialyzed at 4 °C overnight using dialysis membrane (ZelluTrans, Carl Roth 12-14 MWCO). BN-dialysis buffer was the same as BN-lysis buffer with the concentration of detergent reduced to 0.3%.

BN-PAGE. Protein complexes were separated in BN-PAGE (50 µg per well was loaded). NativeMark unstained protein standard (Invitrogen) was used as a marker. BN-PAGE was performed at 4 °C with ServaGel N Native Gel Starter Kit (Serva Electrophoresis) according to the manufacturer's instructions. For BN-PAGE we cut the individual sample gel strips from the entire gel and 5 mm slices of gel strips were prepared. BN-PAGE with molecular mass marker and two to three lanes of the same protein sample were stained by GelCode Stain Reagent (Thermo Scientific), and the molecular mass of the protein complexes in the cut slices was calculated.

Elution of protein complexes from BN-PAGE. We placed gel slices in clean screw-cap microcentrifuge tubes, added 0.5 ml elution buffer (50 mM Tris-HCl, 150 mM NaCl and 0.1 mM EDTA; pH 7.5), incubated tubes in a shaker at 30 °C overnight, centrifuged samples at 10,000g for 10 min and carefully transferred the supernatant into new tubes.

Acetone precipitation of proteins. We added four volumes of ice-cold (–20 °C) acetone to one volume of sample, vortexed the tube, incubated it for 60 min at –20 °C and centrifuged it for 10 min at 15,000g. We then carefully removed supernatant, allowed acetone to evaporate from the uncapped tube at room temperature for 30 min, added 1× Laemmli buffer and boiled the samples at 95 °C for 5 min. We performed SDS-PAGE with the protein samples followed by western blot analysis with the following antibodies: HCLS1 (rabbit, polyclonal, 4503, 1:400, Cell Signaling), LEF-1 (rabbit, monoclonal, clone C18A7, 2286, 1:400, Cell Signaling) and HAX1 (rabbit, polyclonal, sc-28268, 1:250, Santa Cruz).

GST pull-down assay. We washed Jurkat cells (1×10^7) once with ice-cold PBS, pelleted them and added 1 ml Pierce IP lysis buffer (25 mM Tris-HCl, pH 7.4, 150 mM NaCl, 1% Nonident P-40, 1 mM EDTA, 5% glycerol) followed by incubation and periodic mixing for 5 min. Cellular lysate was centrifuged at 13,000g for 10 min at 4 °C to pellet cell debris. We equilibrated the Glutathione HiCap Matrix (Qiagen) using the buffer TN1 (50 mM Tris-HCl, pH 8.0, 200 mM NaCl, 1 mM EDTA, 1% Nonident P-40, 1 mM DTT, 10 mM MgCl₂, protease inhibitor cocktails). We then mixed and centrifuged the beads, removed buffer and resuspended them in 50 µl of fresh TN1 buffer. We preincubated the cell lysate with 100 µl equilibrated Glutathione HiCap Matrix for 2 h at 2–8 °C to remove proteins nonspecifically interacting with the beads. We mixed 70 µg equilibrated Glutathione HiCap Matrix and 10 µg human recombinant HCLS1 GST-tagged protein (Abnova, H00003059-P01) with precleared cell lysate. Before pull-down we dialyzed HCLS1-GST protein against 50 mM Tris-HCl pH 8.0 overnight to remove reduced glutathione (a component of the storage buffer). To check nonspecific binding, we performed pull-down with GST protein (GeneTex, GTX65488) alone. We incubated GST pull-down samples at 4 °C with end-over-end mixing for 4 h, centrifuged at 1,000g for 2 min at 2–8 °C and removed supernatant. The beads were washed three times with TN1 buffer, mixed with 50 µl 2× SDS-PAGE protein sample buffer and boiled at 95 °C for 5 min. To detect proteins associated with the HCLS1-GST-tagged protein, we ran SDS-PAGE and transferred proteins to a nitrocellulose membrane for subsequent western blot analysis with antibodies to LEF-1 and HCLS1.

Duolink *in situ* proximity ligation assay for single proteins and protein-protein interactions in primary CD34⁺ and CD33⁺ cells. The Duolink assay (Olink Bioscience) allows detection of single proteins or endogenous protein interaction through a pair of specific oligonucleotide-conjugated antibodies. Individual proteins or protein interactions are visualized by fluorescent dots (red) of amplified oligonucleotides conjugated to antibodies specific to proteins of interest in the cell. Cells were starved for 12–16 h and treated or untreated with 10 ng/ml of G-CSF (Amgen) *in vitro* for 15 min, and cytospin slides (1×10^4 cells per slide) were made. Cells on the cytospin slides were fixed in ice-cold methanol and permeabilized using 0.1% Triton X-100. Samples were blocked in 1× blocking solution (Olink Bioscience) for 30 min at 37 °C in a humidified chamber. All subsequent incubations were done in a humidified chamber maintained at 37 °C. Cytospins were incubated with different antibody combinations for 1 h. We used mouse antibody to HCLS1 (1:50 dilution, BD Bioscience, 610541), rabbit antibody to LEF-1 (1:50 dilution, Epitomics, 2458-1), mouse antibody to LEF-1 (1:50 dilution, Calbiochem, NA64), rabbit antibody to phospho-HCLS1

(1:50 dilution, Cell Signaling, 45079) and mouse antibody to HAX1 (1:50 dilution, BD Bioscience, 610824). Cytospins were subsequently incubated with anti-mouse PLA–minus and anti-rabbit PLA–plus secondary probes for 45 min. Oligonucleotides complementary to the proximity probe DNA extensions were incubated in 1× hybridization solution for 15 min. To produce the rolling-circle amplification priming template, T4 DNA ligase (1:40) was added to samples, and samples were incubated for 15 min. Rolling-circle amplification of ligated oligonucleotide template was initiated by addition of Phi29 DNA polymerase followed by incubation for 90 min. Finally, Texas red–labeled oligonucleotide detection probes were incubated in 1× detection solution for 60 min. Cells were washed in PBS–T, in 2× SSC, in 0.2× SSC, in 0.02× SSC and in 70% ethanol. All washing procedures and washing solutions are described in the manufacturer's protocol. Samples were air dried and mounted with Olink mounting medium (Olink Bioscience) containing DAPI nuclear stain and examined with a Zeiss Axiovert Imager M1 epifluorescence microscope.

Coimmunoprecipitation. HEK293T cells were transfected with pcDNA–HCLS1 and pcDNA–LEF-1–HA–tag (LEF-1–HA–WT) or pcDNA–LEF-1–Ala16–HA–tag (LEF-1–HA–MUT) using Lipofectamine. 36 h after transfection, cells were lysed with RIPA buffer and LEF-1 protein was immunoprecipitated with protein G agarose beads conjugated with antibody to HA tag (Cell Signaling Technology). Endogenous LEF-1 protein from the Jurkat cell line was immunoprecipitated with protein G agarose beads conjugated with rabbit polyclonal antibody to LEF-1 (R.G.); endogenous HCLS1 protein from primary bone marrow CD34⁺ cells was immunoprecipitated with protein G agarose beads conjugated with rabbit polyclonal antibody to HCLS1 (Cell Signaling Technology) with subsequent washing out of proteins which nonspecifically bound to beads or antibody used for IP. Coimmunoprecipitates of either LEF-1 (with HCLS1 or with HAX1) or HCLS1 (with Lyn and Syk) proteins were eluted from the beads in Laemmli buffer and were detected by western blotting with the respective antibodies as indicated in the methods above for western blotting.

Colony-forming units assay. Human CD34⁺ cells were transduced with lentiviral constructs, as indicated in each experiment; GFP⁺ or RFP⁺ cells were sorted and plated in 1 ml methylcellulose medium (5 × 10³/dish; Methocult H4230; StemCell Technologies) supplemented with 10 ng/ml G–CSF or with cytokine cocktail (10 ng/ml of G–CSF, 10 ng/ml of GM–CSF, 10 ng/ml IL–3, 10 ng/ml of SCF and 1 U of EPO) (R&D Systems). After 14 d of culture, the numbers of CFU–G, CFU–GM and BFU–E colonies were calculated. Mouse bone marrow mononuclear cells were isolated by flushing the long bones with ice–cold PBS. Cells were plated in 1 ml methylcellulose medium (1 × 10⁵ per dish; Methocult M3234; StemCell Technologies) supplemented with 10 ng/ml G–CSF or in methylcellulose medium with cytokine cocktail (Methocult GF M3434; StemCell Technologies). After 14 d of culture, the numbers of CFU–G, CFU–GM and BFU–E colonies were counted.

Cell stimulation, intracellular staining of proteins and analysis by FACS. Serum-starved 293T–GCSFR, CD34⁺ or CD33⁺ cells were incubated with 10 ng/ml of rhG–CSF, washed in ice–cold PBS, fixed in 4% paraformaldehyde for 10 min, permeabilized with 0.5% Triton X–100 for 10 min and incubated with phalloidin–APC (F–actin staining, Invitrogen), rabbit polyclonal antibody to HCLS1 (4503S, 1:500), rabbit polyclonal antibody to phospho–HCLS1 (Tyr397, 4507S, 1:500), rabbit polyclonal antibody to Akt (9272, 1:500), rabbit polyclonal antibody to phospho–Akt (Ser473, 1:500, 9271), rabbit polyclonal antibody to PI3K p85 (4292, 1:500) (all from Cell Signaling Technology) or rabbit polyclonal antibody to phospho–PI3K p85 (Tyr467/Tyr199; Abcam, 1:500, ab63566) for 1 h at 4 °C. Cells were subsequently washed and stained with secondary FITC– or TRITC–conjugated antibody (Molecular Probes) and assessed by a FACSCalibur instrument.

In vitro cell proliferation. AML blasts were isolated from the peripheral blood or bone marrow of patients with AML using Ficoll density centrifugation. We cultured 1 × 10⁵ of transduced and sorted RFP⁺ AML blasts in RPMI 1640 medium supplemented with 10% FCS, 20 ng/ml interleukin–3 (IL–3), 20 ng/ml interleukin–6 (IL–6), 20 ng/ml thrombopoietin (TPO), 50 ng/ml stem cell factor (SCF) and 50 ng/ml Flt3–l (all purchased from R&D Systems). For assessment

of proliferation, we counted viable cells using Trypan blue dye exclusion using a hemocytometer and determined cell proliferation using a luminescence–based cell proliferation kit from Promega. We determined the percentage of apoptotic cells using annexin V–FITC conjugate (Pharmingen).

LEF-1 cDNA synthesis and construction of LEF-1 cDNA and LEF-1 Ala16 cDNA containing lentiviral vectors. We amplified 1220–bp LEF-1 cDNA and cloned it into the pRRL.PPT.SF.i2GFPpre vector. This vector is a derivative of the standard lentiviral vector pRRL.PPT.PGK.GFPpre (provided by L. Naldini)¹. Details are available upon request. To construct LEF-1 with a mutated HCLS1 binding site (LEF-1 Ala16), we replaced residues 186–192 in pRRL.PPT.SF.LEF-1.i2GFPpre with an alanine–glycine sequence using a site–directed mutagenesis kit from Invitrogen.

Promoter constructs and luciferase assays for LEF1, HCLS1, CEBPA and CCND1 gene promoter activity. We cloned human genomic DNA encompassing upstream regions of *LEF1* (3,600 bp) or *HCLS1* (1,600 bp) into a promoter–less luciferase construct, pGL4 Basic (Promega). The *CEBPA* promoter (5,400 bp) in the pGL3 vector was a gift from Q. Tong and the *CCND1* promoter (1,748 bp) was a gift from O. Tetsu. We introduced point mutations into LEF-1–binding sites of *LEF1*, *HCLS1* and *CEBPA* promoter constructs using the QuikChange II XL site–directed mutagenesis kit from Stratagene. Reporter plasmids along with pCMV–Renilla and expression plasmids containing cDNA or shRNA, as indicated in each experiment, were transfected into HEK293T cells using Lipofectamine or into CD34⁺ cells using Gene Pulser MXcell electroporation system and transfection reagent (Bio–Rad) according to the manufacturer's instructions. Transfected CD34⁺ cells were incubated with or without 10 ng/ml of rhG–CSF. After 36 h (for HEK293T cells) or 12 h (for CD34⁺ cells), cells were lysed and assayed with the Dual Luciferase Kit (Promega) according to the manufacturer's instructions. Luminescence was recorded by a Modulo 96 luminometer (Turner Biosystems).

Chromatin immunoprecipitation assays. We cross–linked CD34⁺ cells (1 × 10⁶) in 3.7% formaldehyde for 10 min at room temperature, stopped the cross–linking reaction by adding 0.125 M glycine, rinsed twice in ice–cold PBS with protease inhibitors (Halt protease inhibitor cocktail (100×), Pierce Thermo Scientific, 78429), resuspended in 1 ml of SDS lysis buffer containing protease inhibitors, and incubated for 10 min on ice. We sonicated DNA–protein complexes with three 15–s pulses at 50% of the maximum output using the HD 2070 sonicator from Bandelin Electronic. We set aside one–tenth of the sample for measurement of the input control, precleaned the remaining sample with blocked Staph A cells (Calbiochem, 507858), immunoprecipitated precleaned chromatin using the LEF-1–specific polyclonal antibody and eluted immunoprecipitated protein–DNA complexes. We reversed the cross–links with 0.3 M NaCl at 67 °C for 4 h and deproteinated samples with 20 mg/ml of proteinase K in the presence of 0.5% SDS. We detected LEF-1–associated DNA by PCR amplification using 200 ng of immunoprecipitated DNA or 200 ng of total input, followed by DNA sequencing using the dye terminator method (ABI).

Immunofluorescence staining and confocal microscopy. We stimulated 1 × 10⁴ 293T–G–CSFR cells with 10 ng/ml of rhG–CSF for 5 min, subsequently fixed them in 4% paraformaldehyde for 10 min, permeabilized with 0.5% Triton X–100 for 5 min, incubated with antibody to phalloidin (Invitrogen) for 1 h at 4 °C and assessed staining by confocal microscopy.

Mice. Male *Hcls1*^{–/–} mice on the C57BL/6J background have been described¹⁶. Male WT C57BL/6J mice were obtained from The Jackson Laboratory. All mice were housed under pathogen–free conditions in the Children's Hospital of Philadelphia animal facility. All studies involving animals were reviewed and approved by the Children's Hospital of Philadelphia Institutional Animal Care and Use Committee.

In vitro granulocytic differentiation of mouse bone marrow cells. Mouse bone marrow mononuclear cells were isolated by flushing the long bones with ice–cold PBS. Cells were plated in 1 ml Stemline II hematopoietic stem cell expansion

medium (Sigma) supplemented with 10% FCS and cytokine cocktail (4 ng/ml mIL-3, 10 ng/ml hIL-6, 20 ng/ml hFlt-3L, 40 ng/ml IGF-1, 100 ng/ml mSCF and 1 mM dexamethasone). After 2 d of culture, cells were transduced with lentiviral constructs. After 3 d, transduced cells were placed in differentiation medium (RPMI supplemented with 10% FCS and cytokine cocktail (10 ng/ml hG-CSF, 10 ng/ml mGM-CSF, 5 ng/ml mIL-3, 10 ng/ml hIL-6, R&D Systems) for 7 d and with 10 ng/ml of G-CSF for four more days. The percentage of GFP⁺Gr-1^{hi}CD11b^{hi} mature granulocytes was assessed by FACS.

Lentiviral transduction of CD34⁺ cells, primary blasts from patients with AML and cell lines. We used HEK293T cells for lentiviral supernatant production. HEK293T cells were maintained in DMEM supplemented with 10% FCS, 100 U/ml penicillin-streptomycin, and 2 mM glutamine. On the day before transfection, 5×10^6 HEK293T cells were plated on a 10-cm dish. For transfection, the medium was changed and 25 μ M chloroquine (Sigma-Aldrich, Munich, Germany) was added. Transfer vector DNA (8 μ g) and 5 μ g of VSVg (glycoprotein of the vesicular stomatitis virus) envelope plasmid (A. Schambach) were used. In addition, 12 μ g of a lentiviral Gag/Pol plasmid (pcDNA3 g/p 4xCTE) and 5 μ g of a Rev plasmid (pRSV-Rev, provided by Thomas J. Hope) were co-transfected using the calcium phosphate technique. Medium was changed after 10–12 h. Transfection efficiency was monitored by FACS analysis. Supernatants containing the viral particles were collected 24–72 h after transfection, filtered through a 0.22- μ m filter, concentrated by ultracentrifugation and stored at –80 °C until use. The virus titers averaged and were typically $1-5 \times 10^8$ IU/ml after ultracentrifugation. We transduced CD34⁺ cells from three healthy donors, primary blasts from three patients with AML and the NB4 cell line (2×10^5 per well) with lentiviral supernatants with a multiplicity

of infection of 1–2, retransduced after 24 h and assessed transduction efficiency after 72 h as the percentage of RFP-positive cells.

Sequences of shRNAs. The sequences of the shRNAs are as follows: anti-LEF-1a shRNA: 5'-GATCTTCGCCGAGATCAG-3'; anti-LEF-1b shRNA: 5'-CGACACTTCCATGTCCAG-3'; anti-HCLS1b shRNA: 5'-GACTACAA GGGAGAGACGGAG-3'; anti-HCLS1f shRNA: 5'-GAACCAGAGGGGGACT ATG-3'; anti-HAX1a shRNA 282: 5'-AATAGCATCTTCAGCGATA-3'; anti-HAX1b shRNA 720: 5'-CGGACAGAGACTACAGTAA-3'.

Sequencing of the HCLS1 gene. We isolated DNA from blasts or mononuclear cells from peripheral blood from AML patients or healthy individuals, respectively, using the DNA Isolation Kit from Qiagen. We made primers for amplification of 12 exons with exon-intron boundaries of the HCLS1 gene, optimized PCR and sequencing conditions for each primer pair, amplified exons using PCR, purified PCR products using a QIAquick PCR purification kit from Qiagen (28106) and directly sequenced with the ABI PRISM Dye Terminator Cycle Sequencing Ready Reaction Kit on a 3500 Genetic Analyzer (Applied Biosystems). We analyzed the data using 4peaks software (Mekentosj B.V.) and Chromas software.

Statistical analysis. We performed statistical analysis using the SPSS V. 9.0 statistical package (SPSS) and a two-sided unpaired Student's *t*-test for analysis of differences in mean values between groups.

Additional methods. Additional methodology is described in **Supplementary Methods**.